Ordered Silylation of Layered Silicate RUB-51 with Half-Sodalite Cages

Yusuke Asakura,[1] Yuki Matsuo,[1] Nobuyuki Takahashi,[1] and Kazuyuki Kuroda*[1,2]

[1]Department of Applied Chemistry, Faculty of Science and Engineering, Waseda University,
3-4-1 Ohkubo, Shinjuku-ku, Tokyo 169-8555

[2]Kagami Memorial Research Institute for Materials Science and Technology, Waseda University,
2-8-26 Nishiwaseda, Shinjuku-ku, Tokyo 169-0051

Received May 16, 2011; E-mail: kuroda@waseda.jp

Layered silicate RUB-51 with half-sodalite cages was silylated with dichlorodimethylsilane and trichloromethylsilane. RUB-51, which possesses two confronting Si–O$^-$/Si–OH groups on the interlayer surface, was reacted with bi/tri-functional silylating agents to induce bidentate silylation. RUB-51 silylated with dichlorodimethylsilane was delaminated through ultrasonication in cyclohexane. Layered octosilicate, which also possesses two confronting Si–O$^-$/Si–OH groups to form a bidentate state, was reacted with the same silylating reagents. The comparison of these silylated products derived from two different layered silicates reveals that the structures of silylated interlayer surfaces are varied by the arrangement of the two Si–O$^-$/Si–OH groups. Silylated RUB-51 possesses zigzag grooves on the layer surfaces which will be useful for silicate-based nanomaterials design.

Silicate-based materials possessing ordered frameworks and nanospaces, such as zeolites and layered silicates, have been applied in various fields, such as catalysis, adsorption, and ion exchange. Their functions are affected by various parameters, including composition, structure, size and shape of nanospace, and morphology.[1] Among such parameters, silicate frameworks should be precisely designed for both deeper understanding of the structure–property relationships and creating controlled functionalities. Although hydrothermal synthesis has been utilized to construct crystalline silicate frameworks,[2] it is quite difficult to apply this synthetic method for precise design of silicate structures even though our understanding of the role of structure-directing agents has greatly progressed in recent years.[3] On the other hand, bottom-up approaches are promising for this purpose because various metastable species, which cannot be used in hydrothermal synthesis, can be incorporated into crystalline silicates.

Layered silicates, such as PREFER,[4] kanemite,[5] layered octosilicate,[6] and AMH-3,[7] are composed of SiO_4 tetrahedral units and are quite useful as a framework for topotactic bottom-up approaches. Interlayer Si–O$^-$/Si–OH groups on layered silicates are arranged in ordered manners and are reactive for covalent modifications[8] including interlayer condensation[9] and silylation,[10] while the original silicate frameworks can be retained. We reported the transformation of layered octosilicate into new 2-D and 3-D crystalline siloxane networks through well-ordered silylation with alkoxychlorosilanes.[11] Interestingly, alkoxysilyl groups are immobilized as only Q^2 (Q^n: $O_{4-n}\mathbf{Si}(OSi)_n$) environments (bidentate silylation). The bidentate silylation is realized because confronting Si–O$^-$/Si–OH groups on the interlayer surfaces are closely located and react with one silylating reagent with bifunctionality. Such an ordered modification can precisely control the thickness of silicate layers[11] and the shape and structure of surfaces can be changed. The thickness of silicate layers is important, for example Ogawa et al. reported that the thickness of a layered silicate affects the emission behavior of luminescent cations intercalated in the interlayer spaces.[12] Some layered silicates possess grooves on the surfaces which leads to the formation of micropores through interlayer condensation.[9] At present, bidentate silylation reaction has been achieved only for layered octosilicate[11,13] whose crystal structure has been determined. The use of *alkoxy*silyl groups results in the formation of new layered silicates by the hydrolysis of the alkoxy groups.[11b] If we can expand the variety of layered silicates that can be silylated bidentately, the possibility of designing silicate-based nanomaterials should be enlarged.

Layered silicates RUB-15[14] and RUB-51 (Figure 1)[15] are composed of connecting half-sodalite cages made up of 4- and 6-rings.[16] The stacking sequence of layers of RUB-15 is ABABAB, and that of RUB-51 is AAA. Moteki et al. reported the conversion of RUB-15 into the sodalite structure through treatment with acetic acid and the following calcination (interlayer condensation).[9h] Consequently, the layers of RUB-15 and RUB-51 are useful as building units of new siloxane networks. RUB-51 possesses confronting Si–O$^-$/Si–OH groups arranged on the interlayer surfaces. The distance between the two confronting Si–O$^-$/Si–OH groups is 0.24 nm and the next closest distance between two sets of Si–O$^-$/Si–OH groups is 0.44 nm. Therefore, we expect that RUB-51 can be reacted bidentately with dichloro- or trichlorosilyl groups. Also, the confronting Si–O$^-$/Si–OH groups on the surface of RUB-51 take a "V"-shaped arrangement which is different from that of layered octosilicate.[15] Silylated RUB-51 is expected to have anisotropic grooves on the surfaces composed of grafted silyl groups as the walls. Such formed grooves are interesting because the arrangement of intercalated guest species may be controlled by the interlayer surfaces, and

Published on the web September 3, 2011; doi:10.1246/bcsj.20110143

silylated layers are also potentially useful for the formation of a microporous material by interlayer condensation.

Here we report silylation reactions of RUB-51 with trichloromethylsilane and dichlorodimethylsilane (Scheme 1). Layered silicates are usually ion-exchanged with bulky cations like alkylammonium ions before silylation reactions.[10c] However, the original structures are lost because the interlayer environments and layer sequences are changed.[17] In fact, Iozzi et al. reported a structural change of layered octosilicate by dehydration.[18] In contrast, RUB-51 has natively benzyltrimethylammonium (BTMA) cations in the interlayer space, and has neither metal cations nor water molecules. This is advantageous for direct silylation reaction of RUB-51. In this study, silylating agents possessing the smallest alkyl groups were mainly used as the appropriate reagents for silylation of RUB-51 because organic groups with long-alkyl chains probably prevent a high degree of silylation because of steric hindrance of those groups. Exfoliation of hydrophobic RUB-51 silylated with dichlorodimethylsilane in an organic solvent was then investigated. Exfoliated nanosheets should be applicable for novel and highly efficient catalyst supports[19] and for preparation of polymer nanocomposites.[20]

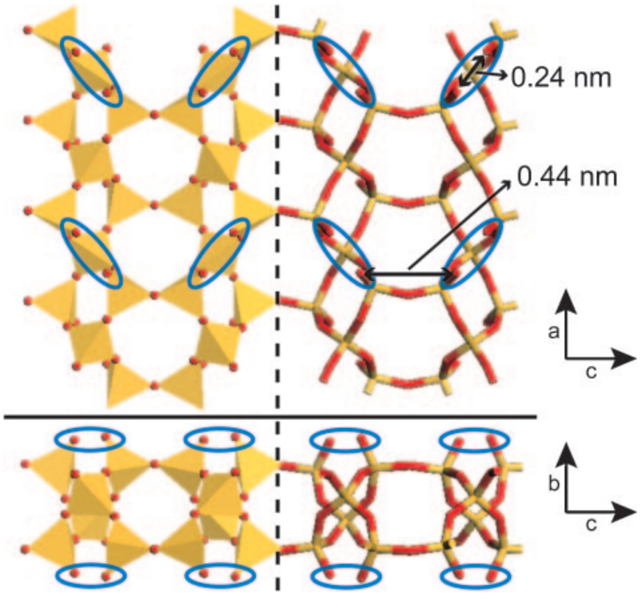

Figure 1. Crystal structure of RUB-51. The ellipsoids indicate confronting Si–O$^-$/Si–OH groups.

Experimental

Materials. Fumed silica (99.8% SiO_2, Aldrich), H_3BO_3 (special grade, 99.5%, Kanto Chem.) and an aqueous solution of BTMA hydroxide (40 wt %, Tokyo Kasei Co.) were used for the preparation of RUB-51. Anhydrous dichloromethane and pyridine (both from Wako Pure Chemical Ltd.) were used for silylation as a solvent and a trapping agent for HCl, respectively. Dichlorodimethylsilane and trichloromethylsilane (both from Tokyo Kasei Co.) were used as silylating agents. All chemicals were used as received.

Synthesis of RUB-51. The synthesis of RUB-51 ($Si_{12}O_{24}(OH)_4[C_6H_5CH_2N(CH_3)_3]_4$) was based on a previous report[15] though seed crystals were added in the starting mixture. SiO_2, H_3BO_3, and aqueous BTMA hydroxide solution (40 wt %) were mixed and stirred to form a gel. The ratio of water in the gel was decreased by evaporation at 60 °C in an oven until the composition ratio of SiO_2:H_3BO_3:BTMAOH:H_2O reached 0.9:0.1:0.5:3–4. Seed crystals of RUB-51 (1 wt % of total SiO_2) were added into the gel to increase the yield of the product. The mixture was treated hydrothermally at 120 °C for 4 weeks in a Teflon-sealed vessel. The solid product was separated by centrifugation, and washed with distilled water and ethanol. The obtained solid was dried in an oven at 70 °C. All powder X-ray diffraction (XRD) peaks of the product (Figure 2a) correspond to those reported in the first report of RUB-51.[15] The solid-state ^{29}Si MAS NMR spectrum of the product (Figure 3a) shows two narrow signals at −101 and −108 ppm corresponding to Q^3 ((O$^-$)**Si**(OSi)$_3$) and Q^4 (**Si**(OSi)$_4$) species, respectively. The intensity ratio of these signals is 2:1, being consistent with that reported previously.[15] The high-resolution SEM image of the product (Supporting Information, Figure S1a) shows a disk-like morphology. The first paper on RUB-51 showed that the presence of B was not detectable.[15] However, the signals of B species were observed in the ^{11}B MAS NMR spectrum of the product (Figure S2). The ^{11}B MAS NMR spectrum of the sample obtained here showed a broad signal in the range from 6 to 15 ppm and one sharp signal at 0 ppm. The former indicates three-coordinated boron and the latter four-coordinated.[21] In general, the signals of boron atoms, coordinating with four O–Si groups (B(OSi)$_4$) in the structures of crystalline solids show signals around −4 ppm.[22] Therefore, it is suggested that the sample does not contain B(OSi)$_4$ sites. Boron atoms of the sample are probably due to amorphous boron silicates. However, the amount of the by-product was

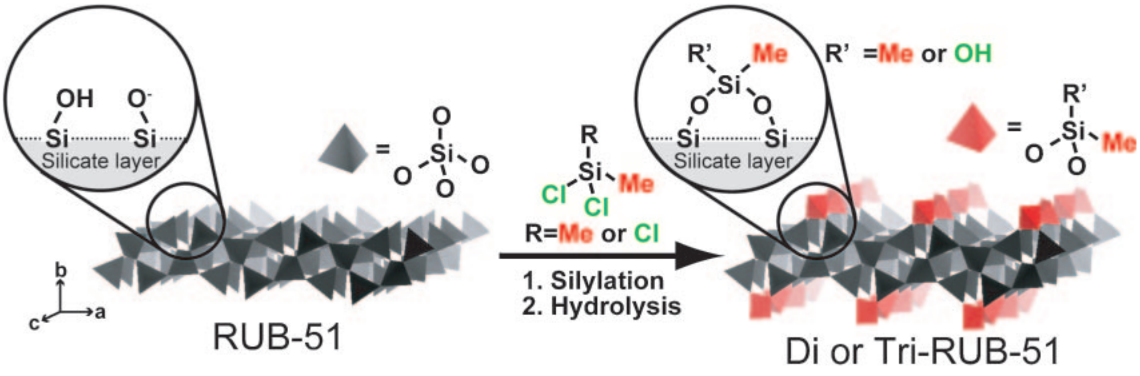

Scheme 1. Silylation of RUB-51 with dichlorodimethylsilane or trichloromethylsilane.

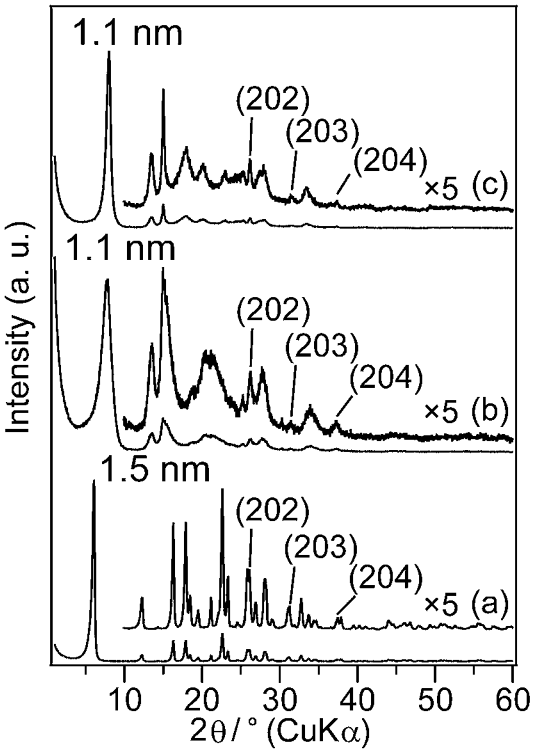

Figure 2. XRD patterns of (a) RUB-51, (b) Di-RUB-51, and (c) Tri-RUB-51.

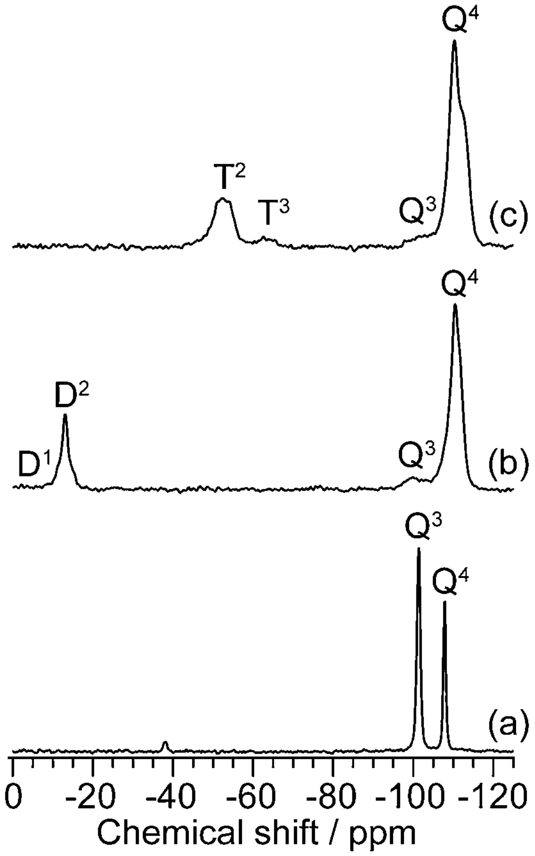

Figure 3. ^{29}Si MAS NMR spectra of (a) RUB-51, (b) Di-RUB-51, and (c) Tri-RUB-51.

low (content of boron was 0.15 wt% by ICP analysis) and the influence of the by-product for characterization is probably small. Therefore, we did not consider the effect of boron species for all the characterization.

Silylation and Subsequent Hydrolysis (Synthesis of Di-RUB-51 or Tri-RUB-51).[13a] RUB-51 (0.5 g), dried in vacuum at 120 °C for 3 h, was dispersed in a mixture of anhydrous dichloromethane (30 mL) and dehydrated pyridine (10 mL). An excess amount (20 equiv of 2 Si–O$^-$/Si–OH groups) of dichlorodimethylsilane or trichloromethylsilane was added to the mixture. They were stirred at room temperature for 1 day under a N_2 flow. They were centrifuged and the obtained slurried samples were washed with dichloromethane. The samples were then treated with a mixture of acetone and H_2O for both the conversion of remaining Si–Cl groups to Si–OH groups and the complete removal of BTMA chloride. The obtained samples were dried under vacuum. The products are denoted as Di-RUB-51 and Tri-RUB-51, respectively.

Exfoliation of Di-RUB-51. Di-RUB-51 (0.020 g) was dispersed in cyclohexane (20 mL). The sample was treated in an ultrasonicator (USS-1, NIHONSEIKI KAISHA Ltd., 35W) for 1 d. Then, the solution was centrifuged at 3500 rpm for 10 min. A small portion of the samples suspended in the supernatant was taken with a TEM grid and observed by scanning electron microscopy. The sample was denoted as Ex-Di-RUB-51.

Characterization. Powder XRD measurements were performed on a Rigaku Rint-Ultima III powder diffractometer with Cu Kα radiation ($\lambda = 0.15418$ nm) by using a parallel beam geometry equipped with a parabolic multilayer solar slit. Solid-state ^{11}B MAS NMR spectra were recorded on a JEOL JNM-ECX-400 spectrometer at a resonance frequency of 128.4 MHz and a recycle delay of 5 s. The samples were put into a 4 mm zirconia rotor and spun at 10 kHz. Solid-state ^{13}C CP/MAS NMR spectra were also recorded on the same spectrometer at a resonance frequency of 100.5 MHz and a recycle delay of 8 s. The samples were put into a 6 mm zirconia rotor and spun at 8 kHz. Solid-state ^{29}Si MAS NMR spectra were also recorded on the same spectrometer at a resonance frequency of 79.42 MHz with a 90° pulse and a recycle delay of 400 s by using a 4 mm zirconia rotor and spinning at 5 kHz. It was confirmed that the signals were fully relaxed under these conditions so that quantitative analysis is possible.[13a] The ^{11}B, ^{13}C, and ^{29}Si chemical shifts were externally referenced to boron trifluoride etherate at 0.0 ppm, hexamethylbenzene at 17.4 ppm (–CH_3) and poly(dimethylsilane) at −33.8 ppm, respectively. The amounts of organic constituents were determined by CHN analysis (Perkin-Elmer, 2400 Series II). Thermogravimetry (TG) measurements were carried out with a Rigaku Thermo Plus 2 instrument under a dry air flow at a heating rate of 10 °C min^{-1}. The scanning electron microscopy (SEM) images were obtained by using a Hitachi S5500 scanning electron microscope. N_2 adsorption–desorption isotherms were measured with a Quantachrome Autosorb-1 instrument at 77 K. The samples were outgassed under vacuum at 120 °C for 3 h prior to the measurement. Brunauer–Emmett–Teller (BET) surface area was calculated from adsorption branch in the relative pressure range from 0.01 to 0.10.

Table 1. Amount of Methyl Groups of the Products

Sample	C /mass %	H /mass %	N /mass %	SiO_2[a] /mass %	Amount of methyl groups /($Si–O^-$ + SiOH)
RUB-51	32.2	4.5	3.8	49.2	—
Di-RUB-51	10.4	2.1	0.1	89.0	0.92
Tri-RUB-51	5.8	1.6	0.0	87.2	—[b]
Heated-Tri-RUB-51[c]	5.1	1.1	0.0	92.3	0.52

a) Residual amount after heating of the sample at 900 °C by TG. The residual SiO_2 contains silyl groups derived from silylating agents. b) The value for Tri-RUB-51 cannot be calculated because of the presence of acetone in the interlayer. c) Tri-RUB-51 was heated at 300 °C for 5 h in air.

Table 2. Relative Intensities in the ^{29}Si MAS NMR Signals of the Products[a]

	D^1	D^2	T^2	T^3	Q^3	Q^4	$(Q^4 - 1)/I$
Chemical shift/ppm:	−3	−13	−52	−63	−101	−108	
RUB-51	—	—	—	—	2	1	—
Di-RUB-51	0.1	0.8	—	—	0.3	2.7	1.9
Tri-RUB-51	—	—	0.8	0.1	0.2	2.8	1.9

a) The total of the relative intensities of Q^3 and Q^4 for each sample is unified to be 3 in order to compare the variation.

Results and Discussion

Silylated Products of RUB-51 (Di-RUB-51 and Tri-RUB-51). SEM images of Di-RUB-51 and Tri-RUB-51 (Figures S1b and S1c, respectively) showed disc-like morphologies and the size of the plates is around 1.0 µm, which reflects the morphology of starting RUB-51. The basal spacings of Di-RUB-51 ($d = 1.1$ nm) and Tri-RUB-51 ($d = 1.1$ nm) decreased from that of RUB-51 (1.5 nm) after silylation (Figure 2). Judging from both the d values and the perpendicular distance (ca. 1.4 nm) between the top of silyl groups on the surface and that on the opposite surface, calculated on the basis of a space-filling model, it is reasonable to propose that the silylated samples take layered structures with interdigitated silyl groups. The XRD patterns of silylated products show that the position of the peak at 37° ($d = 0.24$ nm), attributed to the (204) lattice plane perpendicular to the direction of the silicate layer of RUB-51, does not change before and after the silylation. The peaks due to (202) and (203) also appeared at the same positions. Therefore, the structural regularity of the crystalline silicate layers is retained after silylation.

The complete removal of BTMA ions upon silylation was confirmed by the absence of nitrogen in the silylated products, as verified by the CHN data (Table 1). The amount of methyl groups per set of $Si–O^-$/Si–OH groups of Di-RUB-51 is evaluated to be 0.92 (Table 1), on the basis of the TG and elemental analysis. Ideally, the value of full bidentate silylation should be 1.0. On the other hand, as confirmed by the ^{13}C CP/MAS NMR data (Figure S3c), a certain amount of acetone remained in Tri-RUB-51. Consequently, the ratio of methyl group/($Si–O^-$/Si–OH groups) cannot be correctly calculated. Organic species are occasionally trapped in interlayer spaces above the boiling points.[11b] Because Tri-RUB-51 possesses half-sodalite cups, acetone molecules are probably entrapped in the cups even after drying under vacuum. The major factor of this trapping should be ascribed to the confinement in a restricted space, though hydrogen bonding between carbonyl groups of acetone and silanol groups may contribute to the trapping, which is indicated by the shift of C=O stretching vibration to lower wavenumber.[23] After thermal treatment of Tri-RUB-51 at 300 °C for 5 h (denoted as Heated-Tri-RUB-51; the details (procedure of the heat treatment, SEM image (Figure S4), XRD pattern (Figure S5), ^{29}Si MAS NMR spectrum (Figure S6), the intensity datum (Table S1), and N_2 adsorption and desorption isotherms (Figure S7)) are presented in the Supporting Information), the sample has little acetone in the interlayer, judging from the ^{13}C CP/MAS NMR data (Figure S3d). The value (amount of methyl groups per one set of $Si–O^-$/Si–OH groups) is 0.52 (Table 1), which is approximately consistent with the ideal value for bidentate silylation with trichloromethylsilane (0.5).

The ^{29}Si MAS NMR spectrum of Di-RUB-51 (Figure 3b) shows the decrease of Q^3 signal (Q^3:Q^4 = 0.3:2.7), which indicates that the degree of silylation is ca. 85%. A new signal at −13 ppm, assignable to grafted dimethylsilyl groups with the D^2 ($(CH_3)_2\mathbf{Si}(OSi)_2$) environment, was observed and a very small peak at around −3 ppm due to grafted dimethylsilyl groups with D^1 ($(HO)(CH_3)_2\mathbf{Si}(OSi)$) unit was also observed. The portion of the D^1 signal is much smaller than that of the D^2 signal (less than 10% of total D environments at the largest). In general, $(Q^4 - 1)/I$ (I = units assigned to silylating agents, e.g., D and T environments) means the number of reacted $Si–O^-$/Si–OH groups per silylating agents on the surfaces. When this value is close to 2, silylating agents are immobilized in bidentate state onto silicate layers. The $(Q^4 - 1)/I$ value of Di-RUB-51 is 1.9 (Table 2), strongly indicating the bidentate reaction. The amount of methyl groups of Di-RUB-51 per $Si–O^-$/Si–OH group calculated from the intensity ratio is 0.91. The value is approximately consistent with that calculated from the elemental analysis data (0.92).

In the ^{29}Si MAS NMR spectrum of Tri-RUB-51 (Figure 3c), the silylation led to the significant decrease of the Q^3 signal (Q^3:Q^4 = 0.2:2.8). In addition, a new signal was observed at −52 ppm, assignable to grafted methylsilyl groups with T^2 ($(HO)(CH_3)\mathbf{Si}(OSi)_2$) environment. The intensity of T^3 signal ($(CH_3)\mathbf{Si}(OSi)_3$) (−63 ppm) was much lower than that of T^2.

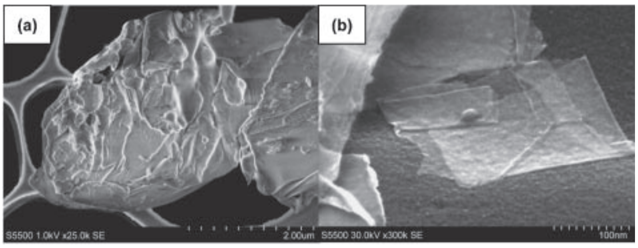

Figure 4. SEM images of Ex-Di-RUB-51, (a) crumpled particles and (b) very thin layered sheets.

There are some possible reasons for the appearance of the T^3 signal. One of the possibilities is due to the *inter*layer condensation between adjacent layers. The second possibility is due to the *intra*layer condensation between remaining Si–OH groups of immobilized silylating agents. The third possibility is due to the reaction of the immobilized silylating reagent with another silylating agent. The intralayer condensation and the reaction of another silylating agent are not plausible, because the crystal structure of RUB-51 suggests that largely separated confronting groups cannot be used for the intralayer condensation and that the dehydrated conditions of silylation can suppress such unwanted reactions among silylating reagents. Hence, the presence of T^3 signal is probably due to the partial interlayer condensation. The $(Q^4 - 1)/I$ value of Tri-RUB-51 is 1.9 (Table 2), indicating the bidentate reaction. In addition, the splitting of Q^4 signal after the silylation means the difference of the environments between the inherent Q^4 units of RUB-51 and the newly formed Q^4 units derived from the Q^3 units through silylation. Judging from the intensity ratio, the larger Q^4 signal at higher magnetic field is probably due to the Si atoms of newly formed Q^4 species from Q^3 by silylation. The splitting of Q^4 units is also observed for silylated layered octosilicate.[11a] All these results are consistant with RUB-51 bidentately silylated with dichlorodimethylsilane and trichloromethylsilane and that the reactivity of trichloromethylsilane is higher than that of dichlorodimethylsilane.

Exfoliation of Di-RUB-51. SEM image of Ex-Di-RUB-51 (Figure 4a) and the bright field STEM (BF-STEM) one (Figure S8) show many crumpled particles. As for the STEM images (Figure S8) thick particles are seen as dark particles, and bright images are taken for thinner samples, if the composition is same. Therefore, it is suggested that the Ex-Di-RUB-51 is thinner than others because Figure S4c shows more particles with relatively small and bright particles, although the particles are found to be aggregated. This behavior indicates delamination and flocculation of layers of Di-RUB-51. RUB-51 possesses a high density of Si–O$^-$/Si–OH groups and the surface of RUB-51 silylated with dichlorodimethylsilane is strongly hydrophobic, as schematically shown in a graphical view of the silylated interlayer surface (Figure S9). As mentioned above, there are a small amount of unsilylated sites but the contribution of these sites to the hydrophobicity should be low. Therefore, the delamination of Di-RUB-51 is probably due to the interaction of the hydrophobic surface with cyclohexane through ultrasonication and the flocculation should occur during the evaporation of the solvent. It should also be noted that very thin layered nanosheets are also observed (Figure 4b), although the ratio of such nanosheets is low. Boucher et al. reported that layered silicate apophyllite with hydrophobic surfaces, prepared by silylation, is exfoliated by a treatment with organic solvents.[24] To the best of our knowledge, this paper is the second reporting the exfoliation or delamination of layered silicates in an organic solvent, although there are some reports of exfoliation or delamination of layered silicates in aqueous systems.[25]

Bidentate Silylation of Interlayer Surfaces. From the viewpoint of precise design of crystalline frameworks of silicates it is quite important to understand the reason for the preference of monodentate or bidentate silylation when the interlayer surfaces are modified with bi- or trifunctional silylating agents. Interlayer condensation after modification also depends on the preference. In order to investigate the factors affecting the bidentate silylation, silylated derivatives of RUB-51 with dichlorodimethylsilane and trichloromethylsilane were compared with those of layered octosilicate (Please see the Supporting Information for the experimental procedure (page 10), ^{29}Si MAS NMR spectra (Figure S10), and the intensity data (Table S2)). As mentioned in the introduction, layered octosilicate and RUB-51 have confronting Si–O$^-$/Si–OH groups arranged on the interlayer surfaces.[5,15] The distances between confronting Si–O$^-$ and Si–OH groups are almost same for both silicates (Please see Figure 1 for RUB-51 (0.24 nm) and Figure S11 for layered octosilicate (0.23 nm)). This means that dichlorosilyl groups can react with both Si–O$^-$ and Si–OH groups to form a bidentate state. In addition, the degree of silylation is nearly equal for both cases. However, the selectivity of bidentate silylation is different. When dichlorodimethylsilane was used, both RUB-51 and layered octosilicate exhibit the presence of immobilized dimethylsilyl groups with a bidentate state. On the other hand, when trichloromethylsilane was used, RUB-51 shows a bidentate state silylation but that of layered octosilicate both monodentate and bidentate states. This difference can be explained by both the arrangement/density of confronting Si–O$^-$/Si–OH groups and the size of functional groups immobilized on the reactive sites on the interlayer surface. Layered octosilicate has lower density of Si–O$^-$/Si–OH groups on the interlayer surface (3.7 groups/nm^2) than that of RUB-51 (4.1 groups/nm^2).[26] Si–O$^-$/Si–OH groups on the surface of RUB-51 take a “V” arrangement, being different from the parallel arrangement of layered octosilicate.

The reason why a mixture of monodentate and bidentate states was observed for the product derived from layered octosilicate and trichloromethylsilane can be explained as follows. Two silylating molecules are thought to be able to approach to one set of confronting Si–O$^-$/Si–OH groups of octosilicate because of their parallel arrangement with lower density. On the other hand, it would be more difficult for two silylating molecules to reach the reaction sites of RUB-51 because the density of Si–O$^-$/Si–OH groups is higher and the direction of the functional groups of the immobilized silylating agents are directed toward the next immobilized groups, which is unlikely to occur because of steric reasons.

When dichlorodimethylsilane is used, layered octosilicate reacts with the silylating agent in a bidentate manner similar to RUB-51. This silylation behavior is probably caused by steric interactions of the silylating agent itself. Because Si–CH_3 is larger than Si–Cl, dichlorodimethylsilane has a slightly larger steric occupancy than trichloromethylsilane. Consequently, two silylating molecules are probably unable to approach to the same reaction site. In fact, we reported that only bidentate silylation occurred in the silylation of layered octosilicate with alkoxytrichlorosilanes having long alkyl chain (carbon number = 6, 8, 10, and 12).[11b] If we look at one silylation site with a more mechanistic view, the preference of monodentate or bidentate after the first grafting may depend on the freedom of conformation of the grafted groups. The bidentate state occurs by a nucleophilic attack[27] of oxygen on a neighboring silanol to immobilized groups with less conformational freedom. On the other hand, the monodentate state will be created by a probable attack of the oxygen on another silylating reagent because of higher conformational freedom of the first grafted silyl groups. The difference in the freedom may arise from the structural and steric variations of both layered silicates and organosilyl groups.

Difference in Silylated Materials Derived from Layered Octosilicate and RUB-51. Functional groups of silylating agents immobilized onto layered octosilicate are directed to the groove of original octosilicate (Please see schematic view, Figure 5a). Therefore, the grooves derived from original octosilicate are occupied by the functional groups of immobilized silylating agents and the new grooves, which are perpendicular to the groove of original octosilicate, are induced (Figure 5b). The size of the groove of silylated octosilicate is almost the same or slightly smaller.

On the other hand, the original form of RUB-51 has connecting half-sodalite cages which provide bumpy surfaces (Figure 5c). Various guest species cannot reach to these surfaces because counter cations are present in the interlayer regions. In general, acid treatment of layered silicates enables us to remove interlayer cations by ion exchange with H^+.[28] However, for the case of RUB-51, the layered structure collapses upon treatment with hydrochloric acid (0.1 M) for 1 d, and a similar finding is reported for various acid treatments of RUB-15.[9h] Therefore, guest species cannot easily access the bumpy interlayer surface. On the other hand, silylated RUB-51 is promising because it has bumpy surfaces without interlayer cations and a collapse is avoided. Therefore, guest species, in particular nonionic species, can reach more easily to the surfaces of silylated RUB-51 than pristine RUB-51 because the electrostatic interactions between the layers are absent in the silylated products. In fact, it is confirmed that Di-RUB-51 shows delamination and flocculation in this study. This finding indicates the intercalation of nonpolar organic substances into the interlayer region of silylated RUB-51, strongly suggesting that the designed surface of Di-RUB-51 is accessible. After silylation of RUB-51, the immobilized silylated groups make uniaxial walls on the surfaces, utilizing the V arrangement of bidentate sites (confronting Si–O^-/Si–OH groups). The schematic view of the walls is shown in Figure 5d. The walls provide uniaxial zigzag grooves. It is known that the grooves of the surface of $K_4Nb_6O_{17}$ single crystal control the orientation of cyanine dye aggregates.[29] Although the size of RUB-51 particle is small, the designed surfaces would induce an arrangement of various guest molecules.

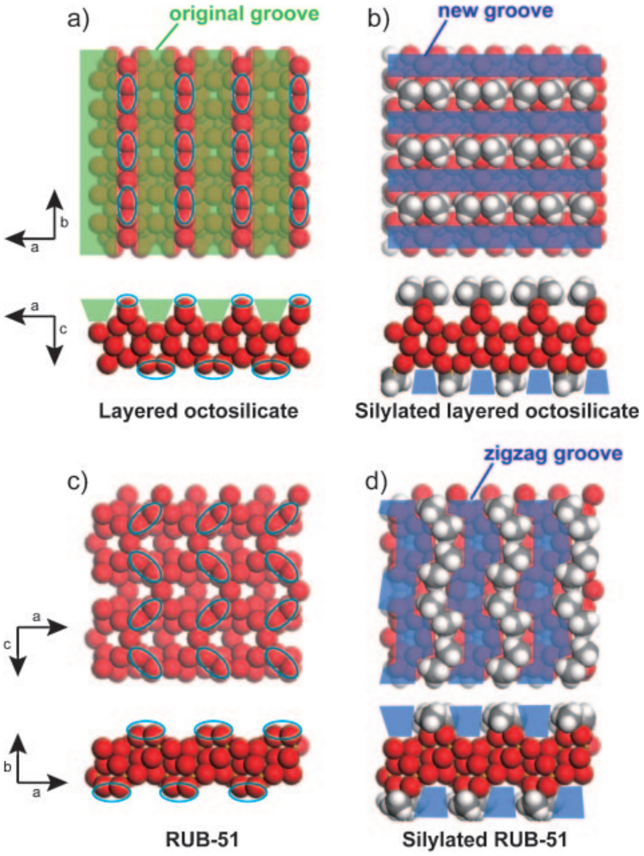

Figure 5. Structual models of (a) layered octosilicate, (b) silylated layered octosilicate, (c) RUB-51, and (d) silylated RUB-51. The models are prepared on the basis of space filling model, using Materials Studio Visualizer (Accelrys K. K.). In this model, 0.135 and 0.026 nm were used as the radii of oxygen and silicon atoms, respectively. The silylated models show ideal bidentate states with dichlorodimethylsilane. The ellipsoids indicate confronting Si–O^-/Si–OH groups. The green regions are original grooves of the starting layered octosilicate. Starting RUB-51 has no grooves. The blue regions are new grooves induced by silylation with dichlorodimethylsilane.

Another point of view on the difference between layered octosilicate and RUB-51 is the variation of formed rings after silylation of confronting reactive sites. As understood by the structural model presented in Figure S12, 5-ring is formed by silylation for octosilicate while 4-ring is formed for RUB-51. The framework of 5-ring is more flexible than 4-ring. In addition, the direction of one functional group out of two bonded on the immobilized silyl groups is essentially perpendicular to the direction of layers.[11b,13a] On the other hand, the direction of two functional groups bonded on the immobilized groups, forming 4-ring, should be inclined to the layer surfaces. This difference indicates that the selection of appropriate layered silicates is quite important to utilize their silylated products as building blocks for silicate-based nanostructural design.

In order to utilize the grooves for the formation of more versatile adsorption sites, it is interesting to examine whether Heated-Tri-RUB-51 has micropores by linking the formed grooves. However, microporosity of Heated-Tri-RUB-51 was not confirmed by nitrogen adsorption data (Figure S7). The reason for very low adsorption of nitrogen is probably because Heated-Tri-RUB-51 possesses a stuffed structure derived from the interdigitated structure, and the pore entrances are supposed to be too small for nitrogen molecules to enter. The interlayer region should be controlled by avoiding the interdigitated structure and by sliding layers by a half-unit cell in the *a* axis to match the convex and concave sites between each layer to form a new microporous channel, which is now under investigation.

It is quite interesting to find the feasibility of this type of silylation with bulkier functional groups for further applications. Our preliminary data suggest that butyltrichlorosilane and trichloro(octyl)silane can directly react with RUB-51. This behavior has not been found for other layered silicates which are usually ion-exchanged with bulky cations like alkylammonium ions before silylation.[10c] The details on the products, including their exfoliation behavior, will be reported in the near future. We have recently found that hexadecyltrimethylammonium ions can be exchanged with benzyltrimethylammonium ions with corresponding expansion of interlayer spaces, which will also be useful for various derivatization of the silicate.

Conclusion

Layered silicate RUB-51 with half-sodalite cages was silylated with dichlorodimethylsilane and trichloromethylsilane. RUB-51 possesses two confronting Si–O$^-$/Si–OH groups and one silylating agent reacted with the two Si–O$^-$/Si–OH groups (bidentate silylation). Layered octosilicate, which is known to form a bidentate state with confronting Si–O$^-$/Si–OH groups on the interlayer surface, was also reacted with the same silylating reagents. The comparison of these silylated products derived from these two different layered silicates indicate that the structures of formed interlayer surfaces are varied by the arrangement of the confronting groups. Silylated RUB-51 possesses unique surfaces composed of uniaxial zigzag grooves. The surface is different from those of other layered silicates. RUB-51 silylated with dichlorodimethylsilane was delaminated and flocculated through ultrasonication in cyclohexane. Therefore, silylation is a quite useful way for the preparation of silicate-based nanomaterials from RUB-51.

We would like to acknowledge Dr. T. Shibue (Materials Characterization Central Laboratory, Waseda University) and Mr. S. Osada (Department of Applied Chemistry, Waseda University) for experimental help. This work was supported in part by the Global COE program "Practical Chemical Wisdom" and Elements Science and Technology Project from MEXT, Japan.

Supporting Information

SEM images of RUB-51, Di-RUB-51, and Tri-RUB-51 (Figure S1), ^{11}B MAS NMR spectrum (Figure S2), ^{13}C CP/MAS NMR spectra of RUB-51, Di-RUB-51, Tri-RUB-51, and Heated-Tri-RUB-51 (Figure S3). Experimental procedure of thermal treatment of Tri-RUB-51 at 300 °C for 5 h, SEM image of Heated-Tri-RUB-51 (Figure S4), XRD pattern of Heated-Tri-RUB-51 (Figure S5), ^{29}Si MAS NMR spectrum of Heated-Tri-RUB-51 (Figure S6), N_2 adsorption–desorption isotherm of Heated-Tri-RUB-51 (Figure S7), relative intensities in the ^{29}Si MAS NMR signal of Heated-Tri-RUB-51 (Table S1). BF-STEM images of RUB-51, Di-RUB-51, and Ex-Di-RUB-51 (Figure S8). Graphic of a hydrophobic sheet of Di-RUB-51 (Figure S9). Experimental procedure of silylation of layered octosilicate, ^{29}Si MAS NMR spectra of silylated octosilicate (Figure S10), relative intensities in the ^{29}Si MAS NMR signals of silylated octosilicate (Table S2). Crystal structure of layered octosilicate (Figure S11). Schematic views of the formation of 5-ring in silylated layered octosilicate and 4-ring in silylated RUB-51 (Figure S12). This material is available free of charge on the Web at: http://www.csj.jp/journals/bcsj/.

References

1 M. E. Davis, *Nature* **2002**, *417*, 813.

2 a) C. S. Cundy, P. A. Cox, *Microporous Mesoporous Mater.* **2005**, *82*, 1. b) G. Lagaly, *Adv. Colloid Interface Sci.* **1979**, *11*, 105.

3 a) A. W. Burton, S. I. Zones, S. Elomari, *Curr. Opin. Colloid Interface Sci.* **2005**, *10*, 211. b) J. Jiang, J. Yu, A. Corma, *Angew. Chem., Int. Ed.* **2010**, *49*, 3120.

4 L. Schreyeck, P. Caullet, J. C. Mougenel, J. L. Guth, B. Marler, *Microporous Mater.* **1996**, *6*, 259.

5 a) L. A. J. Garvie, B. Devouard, T. L. Groy, F. Cámara, P. R. Buseck, *Am. Mineral.* **1999**, *84*, 1170. b) S. Vortmann, J. Rius, B. Marler, H. Gies, *Eur. J. Mineral.* **1999**, *11*, 125.

6 S. Vortmann, J. Rius, S. Siegmann, H. Gies, *J. Phys. Chem. B* **1997**, *101*, 1292.

7 H.-K. Jeong, S. Nair, T. Vogt, L. C. Dickinson, M. Tsapatsis, *Nat. Mater.* **2003**, *2*, 53.

8 N. Takahashi, K. Kuroda, *J. Mater. Chem.* **2011**. doi:10.1039/c1jm10460h.

9 a) L. D. Rollmann, J. L. Schlenker, S. L. Lawton, C. L. Kennedy, G. J. Kennedy, *Microporous Mesoporous Mater.* **2002**, *53*, 179. b) T. Ikeda, Y. Akiyama, Y. Oumi, A. Kawai, F. Mizukami, *Angew. Chem., Int. Ed.* **2004**, *43*, 4892. c) R. Millini, L. C. Carluccio, A. Carati, G. Bellussi, C. Perego, G. Cruciani, S. Zanardi, *Microporous Mesoporous Mater.* **2004**, *74*, 59. d) D. L. Dorset, G. J. Kennedy, *J. Phys. Chem. B* **2004**, *108*, 15216. e) S. Zanardi, A. Alberti, G. Cruciani, A. Corma, V. Fornés, M. Brunelli, *Angew. Chem., Int. Ed.* **2004**, *43*, 4933. f) B. Marler, N. Ströter, H. Gies, *Microporous Mesoporous Mater.* **2005**, *83*, 201. g) Y. X. Wang, H. Gies, B. Marler, U. Müller, *Chem. Mater.* **2005**, *17*, 43. h) T. Moteki, W. Chaikittisilp, A. Shimojima, T. Okubo, *J. Am. Chem. Soc.* **2008**, *130*, 15780.

10 a) E. Ruiz-Hitzky, J. M. Rojo, *Nature* **1980**, *287*, 28. b) E. Ruiz-Hitzky, J. M. Rojo, G. Lagaly, *Colloid Polym. Sci.* **1985**, *263*, 1025. c) T. Yanagisawa, K. Kuroda, C. Kato, *React. Solids* **1988**, *5*, 167. d) M. Ogawa, S. Okutomo, K. Kuroda, *J. Am. Chem. Soc.* **1998**, *120*, 7361. e) A. Shimojima, D. Mochizuki, K. Kuroda, *Chem. Mater.* **2001**, *13*, 3603. f) I. Fujita, K. Kuroda, M. Ogawa, *Chem. Mater.* **2003**, *15*, 3134. g) I. Fujita, K. Kuroda, M. Ogawa, *Chem. Mater.* **2005**, *17*, 3717. h) P. Wu, J. Ruan, L. Wang, L. Wu, Y. Wang, Y. Liu, W. Fan, M. He, O. Terasaki, T. Tatsumi, *J. Am. Chem. Soc.* **2008**, *130*, 8178. i) J. Ruan, P. Wu, B. Slater, Z. Zhao, L. Wu, O. Terasaki, *Chem. Mater.* **2009**, *21*, 2904.

11 a) D. Mochizuki, A. Shimojima, K. Kuroda, *J. Am. Chem. Soc.* **2002**, *124*, 12082. b) D. Mochizuki, A. Shimojima, T. Imagawa, K. Kuroda, *J. Am. Chem. Soc.* **2005**, *127*, 7183.

12 M. Ogawa, Y. Ide, M. Mizushima, *Chem. Commun.* **2010**,

46, 2241.

13 a) D. Mochizuki, S. Kowata, K. Kuroda, *Chem. Mater.* **2006**, *18*, 5223. b) N. Takahashi, H. Hata, K. Kuroda, *Chem. Mater.* **2010**, *22*, 3340.

14 U. Oberhagemann, P. Bayat, B. Marler, H. Gies, J. Rius, *Angew. Chem., Int. Ed. Engl.* **1996**, *35*, 2869.

15 Z. Li, B. Marler, H. Gies, *Chem. Mater.* **2008**, *20*, 1896.

16 L. B. McCusker, F. Liebau, G. Engelhardt, *Pure Appl. Chem.* **2001**, *73*, 381.

17 T. Ikeda, Y. Oumi, T. Takeoka, T. Yokoyama, T. Sano, T. Hanaoka, *Microporous Mesoporous Mater.* **2008**, *110*, 488.

18 M. F. Iozzi, C. Bisio, T. Regi-Macedo, C. Airoldi, M. Cossi, L. Marchese, *J. Mater. Chem.* **2009**, *19*, 2610.

19 S. Nakagaki, M. Halma, A. Bail, G. G. C. Arízaga, F. Wypych, *J. Colloid Interface Sci.* **2005**, *281*, 417.

20 E. P. Giannelis, *Adv. Mater.* **1996**, *8*, 29.

21 R. Martens, W. Müller-Warmuth, *J. Non-Cryst. Solids* **2000**, *265*, 167.

22 a) S.-J. Hwang, C.-Y. Chen, S. I. Zones, *J. Phys. Chem. B* **2004**, *108*, 18535. b) K. Komura, T. Murase, Y. Sugi, M. Koketsu, *Chem. Lett.* **2010**, *39*, 948.

23 A. A. Efremov, A. A. Davydov, *React. Kinet. Catal. Lett.* **1981**, *18*, 353.

24 M. A. Boucher, D. E. Katsoulis, M. E. Kenney, *Chem. Mater.* **2006**, *18*, 360.

25 a) W. J. Roth, J. Čejka, *Catal. Sci. Technol.* **2011**, *1*, 43. In this review, delamination of silicate layers in water is treated in the section of "Synthesis of delaminated materials." b) N. Takahashi, H. Hata, K. Kuroda, *Chem. Mater.* **2011**, *23*, 266. c) B. Zebib, J.-F. Lambert, J. Blanchard, M. Breysse, *Chem. Mater.* **2006**, *18*, 34.

26 The densities of the Si–O^-/Si–OH groups were calculated by counting the number of Si–O^-/Si–OH groups on one side surface within the unit cell.

27 P. Van Der Voort, E. F. Vansant, *J. Liq. Chromatogr. Relat. Technol.* **1996**, *19*, 2723.

28 M. Borowski, O. Kovalev, H. Gies, *Microporous Mesoporous Mater.* **2008**, *107*, 71.

29 N. Miyamoto, K. Kuroda, M. Ogawa, *J. Am. Chem. Soc.* **2001**, *123*, 6949.